https://doi.org/10.5194/hess-2020-611
Preprint. Discussion started: 4 January 2021

Hydrology and Earth System Sciences
Discussions

Comprehensive evaluation of satellite-based and reanalysis soil moisture products using in situ observations over China

Xiaolu Ling [1,3], Ying Huang*[,2,3], Weidong Guo[2,3], Yixin Wang[2], Chaorong Chen[2], Jian Peng [4,5]

[1]School of Environment and Spatial Informatics, China University of Mining and Technology, Xuzhou, 221000, China
[2]Institute for Climate and Global Change Research, School of Atmospheric Sciences, Nanjing University, Nanjing, 210023, China
[3]Joint International Research Laboratory of Atmospheric and Earth System Sciences, Nanjing University, 210023, Nanjing, China
[4] Department of Remote Sensing, Helmholtz Centre for Environmental Research−UFZ, Permoserstrasse 15, 04318, Leipzig, Germany
[5] Remote Sensing Centre for Earth System Research, Leipzig University, 04103, Leipzig, Germany

Correspondence to: Ying Huang (huangy07@nju.edu.cn)

Abstract. Soil moisture (SM) plays a critical role in the water and energy cycles of the earth system; consequently, a long-term SM product with high quality is urgently needed. In this study, five SM products, including one microwave remote sensing product [European Space Agency's Climate Change Initiative (ESA CCI)] and four reanalysis datasets [European Centre for Medium-Range Weather Forecasts (ECMWF) Re-Analysis-Interim (ERAI), National Centers for Environmental Prediction (NCEP), the Twentieth Century Reanalysis Project from National Oceanic and Atmospheric Administration (NOAA) and the European Centre for Medium-Range Weather Forecasts Reanalysis 5 (ERA5)], are systematically evaluated using in situ measurements during 1981-2013 in four climate regions at different timescales over mainland China. The results show that ESA CCI is closest to the observations in terms of both the spatial distributions and magnitude of the monthly SM. All reanalysis products tend to overestimate soil moisture in all regions but have higher correlations than the remote sensing product except in Northwest China. The largest inconsistency is found in southern Northeast China, with a relative RMSE value larger than 0.1. However, none of the products can well reproduce the trends of interannual anomalies. The largest relative bias of 44.6% is found for the ERAI SM product under severe drought conditions, and the lowest relative biases of 4.7% and 9.5% are found for the ESA CCI SM product under severe drought conditions and the NCEP SM product under normal conditions, respectively. As decomposing mean square errors in all the products suggests that the bias terms are the dominant contribution, the ESA CCI SM product is a good option for long-term hydrometeorological applications in mainland China. ERA5 is also a promising product, which is attributed to the incorporation of more observations. This long-term intercomparison study provides clues for SM product enhancement and further hydrological applications.

https://doi.org/10.5194/hess-2020-611
Preprint. Discussion started: 4 January 2021


Hydrology and Earth System Sciences
Discussions

1 Introduction

Soil moisture (SM) is a key state variable in the climate system and controls the exchange of water, energy, and carbon fluxes between the land surface and the atmosphere (Western and Blöschl, 1999; Robock et al., 2000; Ochsner et al., 2013; McColl et al., 2017; Peng and Loew, 2017; Qiu et al., 2018). SM can influence runoff generation, drought development and many other processes of hydrology and agriculture (Markewitz et al., 2010; Das et al., 2011; Sevanto et al., 2014; Akbar et al., 2018). Thus, understanding SM characteristics is beneficial to flood prediction (Komma et al., 2008; Norbiato et al., 2008), drought monitoring (Dai et al., 2004; Anderson et al., 2007; AghaKouchak et al., 2015; Li et al., 2018) and water management, which are directly related to crop growth (Engman, 1991; Bastiaanssen et al., 2000; Dobriyal et al., 2012). SM also affects the climate system through the land-atmosphere feedback loop (Kim and Hong, 2007; Dirmeyer, 2011; Zuo and Zhang, 2016), while the SM-climate interaction actually amplifies climate variability in some transitional climate zones (Seneviratne et al., 2010). Despite the small total mass of SM compared to other water cycle components, it is essential for numerical weather prediction (An et al., 2016) and has been recognized as an essential climate variable (ECV) (GCOS, 2010).

In situ measurements have been acknowledged as the most accurate method to determine SM values, but they cannot fulfill the demand of high spatial and temporal resolution for hydrometeorological use (Bárdossy and Lehmann, 1998). Furthermore, the temporal coverage of in situ measurements is usually not long enough. Therefore, satellite-based products, reanalysis products and numerical model products are often used (Peng et al., 2017). Although model outputs are spatially and temporarily continuous, large uncertainties still exist in model simulations because of the physical structure, parameters, and other reasons (Schellekens et al., 2017). Reanalysis products are generally more accurate, yet they still inherit some uncertainties of the models (Berg et al., 2003), and their spatial resolutions are not high enough for regional application (Crow and Wood, 1999). Despite the short temporal coverage and the limitation of only measuring the surface SM (Petropoulos et al., 2015), satellite-based products are very promising (Chauhan et al., 2003; Bogena et al., 2007; de Jeu et al., 2008) because they are often based on observations with high spatial resolution (Busch et al., 2012). For this reason, satellite-based products are normally taken as reference datasets to evaluate model outputs and reanalysis products (Crow and Ryu, 2009; Lai et al., 2014). To choose the most appropriate SM product for long-term hydrological and meteorological studies, more evaluation work needs to be done. Several evaluation studies have been conducted to find a qualified remote sensing SM product (Li et al., 2009; Zhang et al., 2012; Lai et al., 2014; Peng et al., 2015; An et al., 2016; Ma et al., 2016; Zhu et al., 2018). The SM product from the European Space Agency (ESA) Climate Change Initiative (CCI) program has attracted attention in recent years (Dorigo et al., 2018) and has been proven to have good quality in some regions of the world (Dorigo et al., 2015, 2017; Chakravorty et al., 2016; Ikonen et al., 2018; González-Zamora et al., 2019). Peng et al. (2015) evaluated the ESA CCI product along with four other datasets in Southwest China and found that it has the potential to provide valuable information. Based on observational data and eight model products, An et al. (2016) further confirmed that the CCI SM can be applied over China. Ma et al. (2016) compared the ESA CCI and ERAI products with in situ measurements and found that both products show reliable time-series results.

https://doi.org/10.5194/hess-2020-611
Preprint. Discussion started: 4 January 2021


Hydrology and Earth System Sciences
Discussions

However, no long-term SM products have been compared with the ESA CCI product using in situ measurements, and thus, more in-depth evaluation needs to be done.

Many efforts have been made to assess the reanalysis products of soil variables based on limited observations (Decker et al., 2012). Hagan et al. (2020) found that newer generation reanalysis products have better skill than older generations with higher correlations and lower RMSEs. Analysis of spring SM shows that ERAI can well reproduce the interannual variation in observed value and exhibits a better correlation with precipitation and evaporation than NCEP/NCAR R1, Modern-Era Retrospective analysis for Research and Applications (MERRA), Japan Meteorological Agency and the Central Research Institute of Electric Power Industry (JRA) SM products (Liu et al., 2014). Using in situ observations from 25 networks worldwide from 1979 to 2017, ERA5 SM performs better than other reanalysis products, and NCEP products show higher skill in terms of long-term trends (Li et al., 2020). During weak monsoon conditions, ERAI overestimates SM over India, and SM correlates well with observed rainfall (Shrivastava et al., 2017). Using 670 SM stations worldwide, Deng et al. (2020) found that NCEP performed poorly in December-February and June-August and in arid or temperate and dry climates. Nevertheless, to our knowledge, few studies on the estimation of long time series of SM over mainland China have been conducted.

The objective of this study is to comprehensively evaluate long-term SM products over mainland China and identify the most accurate products for further meteorological and hydrological research. For this purpose, in situ measurements during 1981-2013 are utilized to evaluate five SM products. In addition to the comparison based on different statistical metrics, the source of errors is also discussed.

2 Data and Methodology

2.1 Remotely Sensed and Reanalysis Products

2.1.1 ESA CCI SM

Generated by the ESA Program - Climate Change Initiative CCI project (ESA CCI), ESA CCI SM includes active, passive and combined products (Liu et al., 2012; Gruber et al., 2017). The latest version provides these products based on retrievals of 8 passive and 3 active microwave sensors (Dorigo et al., 2017). The ESA CCI SM v04.4 combined product is employed in this study, which provides SM data starting from November 1978 until now with a spatial resolution of 0.25° plus 0.25°. This version is better at detecting underlying SM changes (Balenzano et al., 2011) than previous versions, as it merges all active and passive Level 2 products directly to generate the combined product (previously, the active and passive products were created separately and then merged) (ESA, 2018). Here, we evaluate all the products over the period from 1981 to 2013 (the same as below), during which in situ measurements are also available.

https://doi.org/10.5194/hess-2020-611
Preprint. Discussion started: 4 January 2021


Hydrology and Earth System Sciences
Discussions

2.1.2 ERAI SM

ERAI is a famous reanalysis product produced by the European Centre for Medium-Range Weather Forecasts (ECMWF, 2009). The data assimilation system is based on the IFS (Cy31r2), which includes a four-dimensional analysis with a 12-hour analysis window. The ERAI data used in this study are on a fixed grid of 80 km and have a temporal resolution of four times daily and monthly. ERAI starts in 1979 and is continuously updated in real time (Paul et al., 2011). ECMWF simulates SM at 4 depths: 0-7 cm, 7-28 cm, 28-100 cm, and 100-255 cm. As suggested by An et al. (2016), the data at depths of 7-28 cm are linearly interpolated to a depth of 10 cm for evaluation.

2.1.3 NCEP SM

NCEP is the 2nd reanalysis product provided by the National Centers for Environmental Prediction and Department of Energy (NCEP-DOE, (Kanamitsu et al., 2002)). The product is available since Jan 1979 with a spatial resolution of approximately 200 km. The temporal resolution includes 4 times daily and monthly data. NCEP has two layers of SM between 0-10 cm and 10-200 cm, in which the first layer was chosen for evaluation.

2.1.4 NOAA SM

The Twentieth Century Reanalysis Project (20CR) led by the Earth System Research Laboratory Physical Sciences Division from the National Oceanic and Atmospheric Administration (NOAA) and the University of Colorado Cooperative Institute for Research in Environmental Sciences (CIRES) also produces a long-term SM product. The version of V2c is used here, spanning the entire twentieth century from 1851 to 2014 (Compo et al., 2011). The NOAA SM product is generated with a spatial resolution of 2 degrees at six hours (also monthly) and with 4 subsurface levels (0, 10, 40, 100 cm), among which the data at 10 cm depth are used.

2.1.5 ERA5 SM

ERA5 is the latest reanalysis product produced by ECMWF, covering the period from 1979 to present. The product uses a new version of the ECMWF assimilation system IFS - IFS Cycle 41R2, which yields hourly analysis fields (C3S, 2017). The spatial (31 km) and temporal (hourly) resolutions of ERA5 are rather high compared to other existing reanalysis datasets. ERA5 will eventually cover the period from 1950 to the present, and one of its key improvements is better SM (Komma et al., 2008). It has more reliable results than ERAI at three sites in Australia. Land surface models driven by ERA5 also show consistent improvements, especially in surface SM, compared to those driven by ERAI (Albergel et al., 2018). Similar to ERAI, ERA5 also has 4 levels of SM data, in which the SM is interpolated to 10 cm for evaluation.

2.2 In Situ SM and Preprocessing of Datasets

The in situ SM observations were generated by three SM datasets as follows:

https://doi.org/10.5194/hess-2020-611
Preprint. Discussion started: 4 January 2021


Hydrology and Earth System Sciences
Discussions

(1) The International Soil Moisture Network (ISMN)

The updated Chinese soil moisture was presented as volumetric soil moisture (θ_v, unit=m^3 m^{-3}) for 1981 to 1999 from the International Soil Moisture Network website (https://ismn.geo.tuwien.ac.at/en/) (Dorigo et al., 2011).

(2) Soil water content from agricultural-meteorological stations

The in situ SM measurements are obtained from the National Meteorological Information Center of China (NMIC, 2006). The data were collected at 778 agricultural-meteorological stations with a temporal resolution of 10 days since May 1991. As there are too many missing observations after 2013, the evaluations of the different datasets are performed until December 2013. There are 7 layers for the in situ observations, and the data at 10 cm depth are utilized. In addition, the observed SM is expressed as the relative water content (θ', unit=%), while the SM in all other products is in the unit of volumetric water content (θ_v, unit=m^3 m^{-3}). Therefore, the observed SM is calculated by:

$$\theta_v = \theta' \times \theta_f \times \rho_b/\rho_w \quad (1)$$

where θ_f is the field capacity, ρ_b is the dry bulk density, and ρ_w is the water density with a value of 1.0 (unit=g cm^{-3}).

(3) Mass percent of measured SM

Another dataset including SM, field capacity and dry bulk density in China was recorded from 1981 to 1998, in which SM was presented as a mass percentage three times each month (Robock et al., 2000) to avoid auxiliary calibration. The volumetric soil moisture is calculated by:

$$\theta_v = \theta_m \times \rho_b/\rho_w \quad (2)$$

in which θ_m is the mass percent of measured soil moisture. Within a certain period, the two parameters of θ_f and ρ_b can be treated as constant. Considering that the field capacity and the dry bulk density are not measured at all stations, data from 119 stations are selected from 1981 to 2013.

The selection of appropriate SM values is based on several criteria. First, if there were multiple data points in the same time period, the ISMN SM value was selected if available, or the average of the remaining two datasets was calculated. Second, SM values greater than 3 times the standard deviation were deleted. All the in situ observations, remote sensing data, and reanalysis data were averaged to monthly data at a depth of 10 cm. The distributions of the available stations are presented in Fig. 1, and detailed information on all the above SM products is listed in Table 1.

2.3 Land Surface Air Temperature, Precipitation, and Radiation

The land surface air temperature and precipitation data are obtained from the National Meteorological Information Center (NMIC) at a spatial resolution of 0.25° spanning from 1961 to the latest (http://data.cma.cn/site/index.html). By interpolating from Chinese ground high density stations (over 2400 observation stations), the CN05.1 dataset includes daily mean temperature, maximum/minimum temperature and precipitation (Wu and Gao, 2013).

The radiation data were downloaded from the China Meteorological Forcing Dataset by merging China Meteorological Administration (CMA) station radiation data estimated from the observed sunshine duration, the World Climate Research

https://doi.org/10.5194/hess-2020-611
Preprint. Discussion started: 4 January 2021


Hydrology and Earth System Sciences
Discussions

Programme's (WCRP) Global Energy and Water Exchanges (GEWEX-SRB) downward shortwave radiation, Princeton forcing data and so on (Yang et al., 2010). The spatial resolution is 1 degree with a 3-hourly temporal resolution.

The self-calibrating Palmer drought severity index (SC-PDSI) was utilized to determine the performance of all products under different drought/well conditions (Wells et al., 2004). By adjusting the climatic characteristics and calculating the duration factors based on the characteristics of the climate at a given location, the SC-PDSI has been widely used in recent decades. The SC-PDSI fit Palmer's 11 categories to allow for comparisons across time and space. A negative value indicates drought conditions, and a positive value indicates a wet spell. The source code to the SC-PDSI can be downloaded via the National Agricultural Decision Support System (NADSS; online at http://nadss.unl.edu/).

2.4 Study Area and Evaluation Strategies

China is located on the eastern coast of Asia, immediately to the west of the Pacific Ocean. It extends roughly from 3.5°N to 53.75°N latitude and from 73.25°E to 135.25°E longitude. Considering climate conditions and the distribution of available SM data, all estimations are conducted in four research regions as suggested by (Ma et al., 2016), which are shown in Fig. 1. Detailed information on the four research regions is specified in Table 2. Figure 1 also shows annual mean precipitation data obtained from 160 Chinese meteorological stations during 1971-2000 from the National Climate Center of China (NCCA). The 30-year averaged annual mean precipitation is treated as the climate mean precipitation to define the division of the climate zone.

To better explain the disagreement between all the SM products and in situ observations, the mean square errors (MSEs) of each product in individual regions are decomposed to quantify the contributions of the correlation term, standard deviation term and bias term.

$$\mathrm{MSE} = 2\sigma_p\sigma_{obs}(1-R) + (\sigma_p - \sigma_{obs})^2 + (\mu_p - \mu_{obs})^2 \quad (2)$$

in which R is the correlation coefficient; σ_p and σ_{obs} are the standard deviations of the products and the observations, respectively; and μ_p and μ_{obs} are the means of the product and the observations, respectively. On the right-hand side of the equation, the first term (correlation term) shows the correspondence between the SM product and the in situ observations. The second term (standard deviation term) explains the degree of similarity of variations, and the third term (bias term) shows the accuracy of the product. With a better understanding of the error structure of the datasets, we can well explain the discrepancy between the SM products and the in situ observations (Dorigo et al., 2010).

3 Results and Discussions

3.1 Spatial Pattern of SM

Figure 2 shows the spatial patterns of the 33-year averaged SM for the in situ observations and five products. Considering the frozen and vegetation cover, only the JJA SM values are used for evaluation. Generally, most SM products are able to capture

https://doi.org/10.5194/hess-2020-611
Preprint. Discussion started: 4 January 2021


Hydrology and Earth System Sciences
Discussions

the spatial distribution of the SM value, although the NOAA SM is always highly overestimated. According to the in situ observations, SM is the lowest in the northwest and increases to the northeast and southeast. Except for NCEP, all the other datasets show two obvious wet centers in China, which are South China and Northwest China. ESA CCI has the highest spatial resolution, followed by ERAI and ERA5, and the spatial resolutions of NCEP and NOAA products are relatively coarse. ESA CCI underestimates SM in northern Northeast China and in Northwest and Southwest China. SM is overestimated by ESA CCI in southern Northeast China and central China, which represents the transitional zone from semihumid regions to semiarid regions. SM is always overestimated for all the analysis datasets, except in Northwest China, where SM is underestimated. For the northwest, ESA CCI always underestimates SM, while other reanalysis datasets always overestimate SM over the whole region. The largest biases reaching 0.15 m^3/m^3 are found in southern Northeast China, and the largest inconsistency is found in the northwest.

The distribution of the relative root mean square error (rRMSE, which is defined as averaged SM observations divided by the RMSE of all SM products) for all stations is shown in Fig. 3 to represent the relative error of the SM dynamical range. Generally, compared to all the reanalysis products, ESA CCI has the lowest rRMSEs, indicating better performance of this remote sensing dataset. Large rRMSEs are found in the Yangtze-Huai region and in the south of Northeast China, which may be attributed to the high SM values. A possible explanation for the poor performance might be that these two regions are strongly influenced by monsoon precipitation.

3.2 Temporal Variability of SM

According to Table 2, all temporal variabilities of SM are averaged over the Northeast China, North China, Yangtze-Huai, and Northwest China regions, which are abbreviated as NE, NC, YH, and NW, respectively, below.

3.2.1 Temporal Evolution

The temporal evolutions of in situ observations and grid point SM values from the five datasets are averaged over each research region during JJA, as displayed in Fig. 4. Generally, all the reanalysis products overestimate the SM, while remote sensing underestimates the SM except for the NE region. All products perform well in the NC region, and the worst performance is found in the NW region. ERAI extremely overestimates SM in all the research regions, while NOAA and NCEP SM has the lowest bias among the reanalysis datasets in the NE and NC regions. Reanalysis can better reproduce the variation characteristics than remote sensing; for example, all reanalyses can reproduce the peak of JJA SM in 1998 in the YH region except for remote sensing.

Table 3 shows biases, RMSEs and correlation coefficients for the comparison between all products and in situ observations during 1981 to 2013. ESA CCI presents the lowest biases and RMSEs for all regions except for the NW region, indicating that ESA CCI is the closest to the observed SM values. The correlation coefficient with observations for ESA CCI is relatively low. Good correlation is obtained for ERA5 SM except in the NW region, indicating that ERA5 can capture the variability well.

https://doi.org/10.5194/hess-2020-611
Preprint. Discussion started: 4 January 2021


Hydrology and Earth System Sciences
Discussions

ERAI SM has the largest positive bias for all regions. All products show a poor performance in correlation in the NW region, implying that the mechanism in this region is not captured by models.

The Taylor diagrams presenting the statistics of the comparison between ESA CCI, NCEP, ERAI, NOAA, ERA5 and in situ observations over four regions are shown in Fig. 5. Most correlation coefficient values are between 0.5 and 0.6 for ERA5, implying a good variability performance. Lower correlations are found for ESA CCI and ERAI SM, demonstrating that both products correlate poorly with the observations. All products exhibit poor correlations in the NW region. Generally, the NOAA SM is always highly overestimated in all regions, and ESA CCI SM is always underestimated.

3.2.2 Seasonality

Figure 6 shows the temporal evolution of SM seasonality averaged spatially over different regions. There exists a negative and a positive bias between remote sensing and reanalysis with respect to SM observations, respectively. The difference in ESA CCI is smaller than all reanalysis products, especially in warm seasons, partly due to different land surface types on satellite measurements, as well as various soil parameters used in the retrieval algorithms (Chakravorty et al., 2016). All reanalysis SM series have a larger dynamic range than in situ observations and remote sensing SM values. ERA5 SM showed a similar variation tendency as the observations, while its bias was larger than that of ERAI, NCEP, and NOAA.

The seasonal cycle of SM in the NE region is obvious, partly due to the land surface vegetation types. The observed SM in all regions decreases from January, reaches its minimum from April to June, and then increases to its maximum from July to September, which can be reproduced by ERAI, NOAA and ERA5. ESA CCI and NCEP are closer to the observations in all regions, while the smallest biases occur in warm seasons and cold seasons for ESA CCI and NCEP, respectively. Additionally, ERAI and ERA5 can both reproduce the trend of SM, but the bias is smaller for ERA5. ESA CCI yields the worst seasonal cycle results considering the changing tendency, especially in cold seasons, which may be because of snow or frozen soil during these periods.

Figure 7 displays the autocorrelation coefficients lagging one month in different seasons to investigate the persistence of the soil moisture anomaly for in situ observations and four analysis datasets. The ESA CCI correlation is not taken into account because of missing values. It is shown from observations that the autocorrelation in spring and autumn is more noticeable than that in summer and winter, partly due to the influences of liquid and solid precipitation and frozen soil. The lowest autocorrelation coefficient is found in the NW region, possibly because of the particular soil type and soil texture there. The regions with good persistence of soil anomalies are located in the northwest and eastern northeast regions of China, which are dominated by relatively simple land cover, for example, bare soil and forests, respectively. The NOAA SM shows larger autocorrelations for all seasons than other reanalysis products, implying that NOAA models should take into account the influence of some other variables on soil moisture in the future, for example, temperature and precipitation. All reanalysis SM data show greater autocorrelation in winter except for the NCEP SM data, indicating better performance of NCEP during cold seasons. ERA5 shows better performance than ERAI, especially with a close autocorrelation coefficient in the NE region.

https://doi.org/10.5194/hess-2020-611
Preprint. Discussion started: 4 January 2021


Hydrology and Earth System Sciences
Discussions

245 **3.2.3 Interannual Anomalies**

SM shows evident interannual anomalies in all the research regions, as shown in Fig. 8. Most peaks and troughs can be well represented by all products in the NE region, while the variation characteristics cannot be reproduced in the other regions, especially in the YH region. Furthermore, all products have a smaller amplitude of variation than observations in extreme wet or drought years in the NC and NW regions.

250 Specifically, the variation range of the observed SM is larger than those of NOAA and ESA CCI, and the range in ERAI is the smallest. Taking the years of drought from 2001 to 2002 and the wet year of 2003 as examples, this characteristic was missed by ESA CCI. The variation range of NCEP SM is significantly smaller than the actual measurement, and the simulation of NCEP is obviously inferior to the other three products.

In the NC region, all products fail to capture the SM variation tendency, especially during extreme drought and wet periods.

255 NOAA and ERA5 can capture the basic trend, but the variation range does not match the measured value. The variation amplitudes of NCEP and ERAI are obviously smaller than the observations.

In the YH region, ERAI and ERA5 can roughly reproduce the trend of change, but the magnitude of the change is large. There are three SM peaks occurring in 1993, 1998 and 2003 in the YH region, in accordance with the 1993 East China Flood, the 1998 Massive Flood and the 2003 Huai River Flood, respectively. These peaks can be reproduced by the ERAI and ERA5

260 datasets.

In the NW region, none of these products are able to reproduce the variation characteristics, especially with worse performance in drought periods than in wet periods. According to the correlation (in Table 3), ERA5 has the best performance, but it shows a fictitious increase from 1981 to 1993.

Generally, ERA5 is of the best quality, with the simulation in NE and NC regions passing the 0.05 significance test. Available

265 data in the NC, YH and NW regions before 1995 are missing for ESA CCI, which might be a possible reason for the poor performance. NCEP has a smaller overall change in SM than observations, and all the datasets exhibit certain weaknesses in representing the interannual variation in SM.

3.3 Decomposition of the Mean Square Error (MSE)

The comprehensive performance of the five products over the four regions from 1981 to 2013 is evaluated. The contribution

270 to MSE is decomposed into a correlation term, standard deviation term and bias term according to Eq. (2). As shown in Fig. 9, the contribution of the bias term is much larger than the correlation term for the ERAI and NCEP SM data in all regions, indicating that reducing biases for both products is the direction we need to follow to further improve the quality of SM products.

The MSE of ESA CCI SM is the smallest for all regions and that of ERA5 is the second smallest in the NC and NW regions.

275 The large correlation term of ESA CCI and NOAA is found in all regions, pointing to the need for improving the capacity of changing variations. Additionally, all products present poor performance in the NW region with a high correlation term. By

https://doi.org/10.5194/hess-2020-611
Preprint. Discussion started: 4 January 2021


Hydrology and Earth System Sciences
Discussions

decomposing the MSE, we can see that in addition to the NW region, ESA CCI has a larger correlation term than the bias term, implying that the main error of ESA CCI comes from the poor performance of the variation tendency. The ERA5 SM dataset performs inconsistently in that its main difference comes from the correlation term in the NC and NW regions, while the bias terms are dominant in the NE and YH regions. Furthermore, the standard deviation term has little effect on MSE for all datasets except for the NCEP product in the NC region. Time series and seasonal cycles of SM of ESA CCI and ERA5 have the highest correlation with the in situ measurements and the lowest MSE in the NC and NW regions. The NOAA SM product also shows a small MSE except in the NW regions, which is similar to former evaluations in some other regions (Peng et al., 2015; An et al., 2016; Zhu et al., 2018).

3.4 SM Performance Under Various Climate Background

Figure 10 shows the averaged relative bias under different humid/arid conditions. The SC-PDSI is utilized (Wells et al., 2004). The relative bias was calculated as the bias of SM products and the in situ observations to be divided by the in situ observations under different conditions. The ESA CCI SM data showed a positive relative bias under severe drought conditions but a negative relative bias under severe wet and normal conditions. The NCEP and NOAA SM data have smaller relative biases under severe wet conditions, while ERAI and ERA5 SM data perform better under normal conditions. The largest difference is found for the ERAI products under severe drought conditions, with an average relative bias of 44.6%. The best performance is found for ESA CCI SM under severe drought conditions and NCEP SM under severe wet conditions, with averaged relative biases of 4.7% and 9.5%, respectively. For the performance in different regions (Fig. 11), the relative bias of all SM products in the NE region is noticeably high, partly due to the various land cover types in this region. The averaged relative bias for ESA CCI under drought conditions is smaller than that under better conditions. Although ERAI and ERA5 always highly overestimate the SM value, they show better performance in the NW region, especially under dry conditions. The smallest relative biases are found for the ESA CCI and NCEP SM products during all conditions.

Figure 12 shows scatter plots of (a) precipitation, (b) temperature, and (c) radiation anomalies versus observed SM anomalies over different regions. Obvious positive/negative correlations are found between precipitation/temperature and SM in the NE and NC regions, respectively. The correlation between net radiation and SM (Fig. 12c) is low, which is partly due to the combined influence of longwave and shortwave radiation. The correlation coefficient is low for all meteorological variables in the NW region, which may be attributed to the special soil type there.

In the winter, SM decreases in all regions mainly because of decreased precipitation. Lower evaporation caused by sudden cooling may explain why SM increases in early winter. SM reaches a local minimum in the spring in most of the regions except the NE region, as a temperature rise leads to higher evaporation, while precipitation does not increase much in this season. In the NE region, ice and snow melting partially compensates for soil water loss and helps maintain a relatively stable SM. Increased precipitation in the summer gives rise to an evident increase in SM. In the autumn, SM continues to increase in the YH and NC regions, which might be attributed to lower evaporation caused by lower temperatures.

https://doi.org/10.5194/hess-2020-611
Preprint. Discussion started: 4 January 2021


Hydrology and Earth System Sciences
Discussions

ERA5 (~0.28125°) has a higher spatial resolution than ERAI (~0.75°), which can be directly reflected in their spatial patterns of SM distribution. ERA5 can well reproduce the spatial distribution and time series of SM over mainland China with high correlations with observations. Looking at the monthly variation in the SM and interannual variation in the SM anomaly, ERA5 has better performance than ERAI. It is proposed that ERA5 will eventually replace ERAI, and we do see improvements in the ERA5 product. However, ERA5 overcorrects the problem of small variation in ERAI, which leads to unrealistically large standard deviations in ERA5 that affect its accuracy. Therefore, more improvements are still needed to improve the quality of the ERA5 SM product.

4 Conclusions

To evaluate the performance of long-term SM products over mainland China, one satellite-based product and four reanalysis datasets from 1981 to 2013 are selected for comparison with in situ measurements at different time scales.

Overall, ESA CCI has the best performance with the highest spatial resolution and accuracy, making it a good option for long-term hydrometeorological applications in China. The 0.25°*0.25° resolution of the ESA CCI product produces the finest spatial pattern of SM, making it more beneficial for regional application than other SM products. However, ESA CCI is not useful because of its poor correlation and missing values, especially in Northeast China.

ERAI and ERA5 can well reproduce the tendency of the time series and perform best at stations, but they overestimate the seasonal variation in SM. ERA5 is also a promising product with better performance in several aspects than ERAI, highlighting the importance of incorporating more observations at finer spatial resolution.

NCEP cannot reproduce the spatial pattern of SM in China, the time series of NCEP SM data is poorly correlated with observations, and the variation amplitude of its seasonal cycle is much larger than that of the observations. NOAA is able to reproduce the basic spatial pattern, but it systematically overestimates SM in China and shows little seasonal variation. All the SM products used in the present study cannot adequately simulate the interannual variation in the SM anomaly.

The mismatch between SM layers in analysis products and observations, as well as their spatial mismatch, should be investigated in the future (Choi and Hur, 2012; Crow et al., 2012). Furthermore, subdaily SM model products considering the advantages of individual models under different weather regimes and climate scenarios would be merged in future work (Chen and Yuan, 2020).

Data Availability. We acknowledge the data providers of the following SM products: ESA CCI (http://www.esa-soilmoisture-cci.org), ECMWF ERAI (https://apps.ecmwf.int/datasets/data/interim-full-daily/levtype=sfc/), ERA5 (https://apps.ecmwf.int/data-catalogues/era5/?class=ea), NCEP (doi:10.1175/BAMS-83-11-1631), NOAA (doi:10.1002/qj.776) and NMIC (http://data.cma.cn/data/cdcdetail/dataCode/AGME_AB2_CHN_TEN.html). The radiation

dataset used in this study was developed by the Data Assimilation and Modeling Center for Tibetan Multi-spheres, Institute of Tibetan Plateau Research, Chinese Academy of Sciences.

Author Contribution. YH, WG, and JP designed the study and performed the experiments; XL and YW performed the experiments, analyzed the data, and wrote the manuscript.

Competing Interests. The authors declare that they have no conflict of interest.

Acknowledgements. This work was jointly supported by the National Key R&D Program of China (2017YFA0603803), National Science Foundation of China (Grant No. 41705101, 41775075), and ESA MOST Dragon 5 programme (Monitoring and Modelling Climate Change in Water, Energy and Carbon Cycles in the Pan-Third Pole Environment, CLIMATE-Pan-TPE).

References

AghaKouchak, A., Farahmand, A., Melton, F. S., Teixeira, J., Anderson, M. C., Wardlow, B. D., and Hain, C. R.: Remote sensing of drought: progress, challenges and opportunities, Rev. Geophys., 53, 452–480, https://doi.org/10.1002/2014rg000456, 2015.

Akbar, R., Gianotti, D. J. S., McColl, K. A., Haghighi, E., Salvucci, G. D., and Entekhabi, D.: Estimation of landscape soil water losses from satellite observations of soil moisture, J. Hydrometeorol., 19, 871–889, https://doi.org/10.1175/jhm-d-17-0200.1, 2018.

Albergel, C., Dutra, E., Munier, S., Calvet, J. C., Munoz-Sabater, J., de Rosnay, P., and Balsamo, G.: ERA-5 and ERA-interim driven ISBA land surface model simulations: which one performs better?, Hydrol. Earth Syst. Sci., 22, 3515–3532, https://doi.org/10.5194/hess-22-3515-2018, 2018.

An, R., Zhang, L., Wang, Z., Quaye-Ballard, J. A., You, J., Shen, X., Gao, W., Huang, L., Zhao, Y., and Ke, Z.: Validation of the ESA CCI soil moisture product in China, Int. J. Appl. Earth Obs. Geoinf., 48, 28–36, https://doi.org/10.1016/j.jag.2015.09.009, 2016.

Anderson, M. C., Norman, J. M., Mecikalski, J. R., Otkin, J. A., and Kustas, W. P.: A climatological study of evapotranspiration and moisture stress across the continental United States based on thermal remote sensing: 2. Surface moisture climatology, J. Geophys. Res., 112, D11112, https://doi.org/10.1029/2006jd007507, 2007.

Balenzano, A., Mattia, F., Satalino, G., and Davidson, M. W. J.: Dense temporal series of C- and L-band SAR data for soil moisture retrieval over agricultural crops, IEEE J. Sel. Top. Appl. Earth Obs. Remote Sens., 4, 439–450, https://doi.org/10.1109/jstars.2010.2052916, 2011.

Bárdossy, A., and Lehmann, W.: Spatial distribution of soil moisture in a small catchment. Part 1: geostatistical analysis, J. Hydrol., 206, 1–15, https://doi.org/10.1016/s0022-1694(97)00152-2, 1998.

https://doi.org/10.5194/hess-2020-611
Preprint. Discussion started: 4 January 2021

Bastiaanssen, W. G. M., Molden, D. J., and Makin, I. W.: Remote sensing for irrigated agriculture: examples from research and possible applications, Agric. Water Manag., 46, 137–155, https://doi.org/10.1016/s0378-3774(00)00080-9, 2000.

Berg, A. A., Famiglietti, J. S., Walker, J. P., and Houser, P. R.: Impact of bias correction to reanalysis products on simulations of North American soil moisture and hydrological fluxes, J. Geophys. Res., 108, 4490, https://doi.org/10.1029/2002jd003334, 2003.

Bogena, H. R., Huisman, J. A., Oberdörster, C., and Vereecken, H.: Evaluation of a low-cost soil water content sensor for wireless network applications, J. Hydrol., 344, 32–42, https://doi.org/10.1016/j.jhydrol.2007.06.032, 2007.

Busch, F. A., Niemann, J. D., and Coleman, M.: Evaluation of an empirical orthogonal function-based method to downscale soil moisture patterns based on topographical attributes, Hydrol. Process., 26, 2696–2709, https://doi.org/10.1002/hyp.8363, 2012.

ERA5: fifth generation of ECMWF atmospheric reanalyses of the global climate: https://cds.climate.copernicus.eu/cdsapp#!/home, last access: 12 July 2018, 2017.

Chakravorty, A., Chahar, B. R., Sharma, O. P., and Dhanya, C. T.: A regional scale performance evaluation of SMOS and ESA-CCI soil moisture products over India with simulated soil moisture from MERRA-Land, Remote Sens. Environ., 186, 514–527, https://doi.org/10.1016/j.rse.2016.09.011, 2016.

Chauhan, N. S., Miller, S., and Ardanuy, P.: Spaceborne soil moisture estimation at high resolution: a microwave-optical/IR synergistic approach, Int. J. Remote Sens., 24, 4599–4622, https://doi.org/10.1080/0143116031000156837, 2003.

Chen, Y., and Yuan, H.: Evaluation of nine sub-daily soil moisture model products over China using high-resolution in situ observations, J. Hydrol., 588, 125054, https://doi.org/10.1016/j.jhydrol.2020.125054, 2020.

Choi, M., and Hur, Y.: A microwave-optical/infrared disaggregation for improving spatial representation of soil moisture using AMSR-E and MODIS products, Remote Sens. Environ., 124, 259–269, https://doi.org/10.1016/j.rse.2012.05.009, 2012.

Compo, G. P., Whitaker, J. S., Sardeshmukh, P. D., Matsui, N., Allan, R. J., Yin, X., Gleason, B. E., Vose, R. S., Rutledge, G., Bessemoulin, P., Brönnimann, S., Brunet, M., Crouthamel, R. I., Grant, A. N., Groisman, P. Y., Jones, P. D., Kruk, M. C., Kruger, A. C., Marshall, G. J., Maugeri, M., Mok, H. Y., Nordli, Ø., Ross, T. F., Trigo, R. M., Wang, X. L., Woodruff, S. D., and Worley, S. J.: The twentieth century reanalysis project, Q. J. R. Meteorol. Soc., 137, 1–28, https://doi.org/10.1002/qj.776, 2011.

Crow, W. T., and Wood, E. F.: Multi-scale dynamics of soil moisture variability observed during SGP'97, Geophys. Res. Lett., 26, 3485–3488, https://doi.org/10.1029/1999gl010880, 1999.

Crow, W. T., and Ryu, D.: A new data assimilation approach for improving runoff prediction using remotely-sensed soil moisture retrievals, Hydrol. Earth Syst. Sci., 13, 1–16, https://doi.org/10.5194/hess-13-1-2009, 2009.

Crow, W. T., Berg, A. A., Cosh, M. H., Loew, A., Mohanty, B. P., Panciera, R., de Rosnay, P., Ryu, D., and Walker, J. P.: Upscaling sparse ground-based soil moisture observations for the validation of coarse-resolution satellite soil moisture products, Rev. Geophys., 50, RG2002, https://doi.org/10.1029/2011rg000372, 2012.

https://doi.org/10.5194/hess-2020-611
Preprint. Discussion started: 4 January 2021


Hydrology and Earth System Sciences
Discussions

Dai, A., Trenberth, K. E., and Qian, T.: A global dataset of palmer drought severity index for 1870–2002: relationship with soil moisture and effects of surface warming, J. Hydrometeorol., 5, 1117–1130, https://doi.org/10.1175/jhm-386.1, 2004.

Das, N. N., Entekhabi, D., and Njoku, E. G.: An algorithm for merging SMAP radiometer and radar data for high-resolution soil-moisture retrieval, IEEE Trans. Geosci. Remote Sens., 49, 1504–1512, https://doi.org/10.1109/tgrs.2010.2089526, 2011.

de Jeu, R. A. M., Wagner, W., Holmes, T. R. H., Dolman, A. J., van de Giesen, N. C., and Friesen, J.: Global soil moisture patterns observed by space borne microwave radiometers and scatterometers, Surv. Geophys., 29, 399–420, https://doi.org/10.1007/s10712-008-9044-0, 2008.

Decker, M., Brunke, M. A., Wang, Z., Sakaguchi, K., Zeng, X., and Bosilovich, M. G.: Evaluation of the reanalysis products from GSFC, NCEP, and ECMWF using flux tower observations, J. Clim., 25, 1916–1944, https://doi.org/10.1175/jcli-d-11-00004.1, 2012.

Deng, Y., Wang, S., Bai, X., Wu, L., Cao, Y., Li, H., Wang, M., Li, C., Yang, Y., Hu, Z., Tian, S., and Lu, Q.: Comparison of soil moisture products from microwave remote sensing, land model, and reanalysis using global ground observations, Hydrol. Process., 34, 836–851, https://doi.org/10.1002/hyp.13636, 2020.

Dirmeyer, P. A.: The terrestrial segment of soil moisture-climate coupling, Geophys. Res. Lett., 38, L16702, https://doi.org/10.1029/2011gl048268, 2011.

Dobriyal, P., Qureshi, A., Badola, R., and Hussain, S. A.: A review of the methods available for estimating soil moisture and its implications for water resource management, J. Hydrol., 458-459, 110–117, https://doi.org/10.1016/j.jhydrol.2012.06.021, 2012.

Dorigo, W., Wagner, W., Albergel, C., Albrecht, F., Balsamo, G., Brocca, L., Chung, D., Ertl, M., Forkel, M., Gruber, A., Haas, E., Hamer, P. D., Hirschi, M., Ikonen, J., de Jeu, R., Kidd, R., Lahoz, W., Liu, Y. Y., Miralles, D., Mistelbauer, T., Nicolai-Shaw, N., Parinussa, R., Pratola, C., Reimer, C., van der Schalie, R., Seneviratne, S. I., Smolander, T., and Lecomte, P.: ESA CCI soil moisture for improved earth system understanding: state-of-the art and future directions, Remote Sens. Environ., 203, 185–215, https://doi.org/10.1016/j.rse.2017.07.001, 2017.

Dorigo, W., Wagner, W., Gruber, A., Scanlon, T., Hahn, S., Kidd, R., Paulik, C., Reimer, C., van der Schalie, R., and de Jeu, R.: ESA soil moisture climate change initiative (soil_moisture_cci): version 04.2 data collection, Cent. Environ. Data Anal., https://doi.org/10.5285/3a8a94c3fa464d68b6d70df291afd457, 2018.

Dorigo, W. A., Scipal, K., Parinussa, R. M., Liu, Y. Y., Wagner, W., de Jeu, R. A. M., and Naeimi, V.: Error characterisation of global active and passive microwave soil moisture datasets, Hydrol. Earth Syst. Sci., 14, 2605–2616, https://doi.org/10.5194/hess-14-2605-2010, 2010.

Dorigo, W. A., Wagner, W., Hohensinn, R., Hahn, S., Paulik, C., Xaver, A., Gruber, A., Drusch, M., Mecklenburg, S., van Oevelen, P., Robock, A., and Jackson, T.: The international soil moisture network: a data hosting facility for global

https://doi.org/10.5194/hess-2020-611
Preprint. Discussion started: 4 January 2021


Hydrology and Earth System Sciences
Discussions

in situ soil moisture measurements, Hydrol. Earth Syst. Sci., 15, 1675–1698, https://doi.org/10.5194/hess-15-1675-2011, 2011.

Dorigo, W. A., Gruber, A., De Jeu, R. A. M., Wagner, W., Stacke, T., Loew, A., Albergel, C., Brocca, L., Chung, D., Parinussa, R. M., and Kidd, R.: Evaluation of the ESA CCI soil moisture product using ground-based observations, Remote Sens. Environ., 162, 380–395, https://doi.org/10.1016/j.rse.2014.07.023, 2015.

ECMWF: European Centre for Medium-Range Weather Forecasts (ECMWF) Re-Analysis Interim (ERA-Interim) Model Data, NCAS British Atmospheric Data Centre, Oxford, UK, 2009.

Engman, E. T.: Applications of microwave remote sensing of soil moisture for water resources and agriculture, Remote Sens. Environ., 35, 213–226, https://doi.org/10.1016/0034-4257(91)90013-v, 1991.

v05.2 release: ESA CCI SM now including SMAP data!: https://www.esa-soilmoisture-cci.org/, last access: 7 September 2018, 2018.

GCOS, 2010. Essential Climate Variables-Land. https://public.wmo.int/en/programmes/global-climate-observing-system/essential-climate-variables.

González-Zamora, Á., Sánchez, N., Pablos, M., and Martínez-Fernández, J.: CCI soil moisture assessment with SMOS soil moisture and in situ data under different environmental conditions and spatial scales in Spain, Remote Sens. Environ., 225, 469–482, https://doi.org/10.1016/j.rse.2018.02.010, 2019.

Gruber, A., Dorigo, W. A., Crow, W., and Wagner, W.: Triple collocation-based merging of satellite soil moisture retrievals, IEEE Trans. Geosci. Remote Sens., 55, 6780–6792, https://doi.org/10.1109/tgrs.2017.2734070, 2017.

Hagan, D. F. T., Parinussa, R. M., Wang, G., and Draper, C. S.: An evaluation of soil moisture anomalies from global model-based datasets over the people's republic of China, Water, 12, 117, https://doi.org/10.3390/w12010117, 2020.

Ikonen, J., Smolander, T., Rautiainen, K., Cohen, J., Lemmetyinen, J., Salminen, M., and Pulliainen, J.: Spatially distributed evaluation of ESA CCI soil moisture products in a northern boreal forest environment, Geosciences, 8, 51, https://doi.org/10.3390/geosciences8020051, 2018.

Kanamitsu, M., Ebisuzaki, W., Woollen, J., Yang, S. K., Hnilo, J. J., Fiorino, M., and Potter, G. L.: NCEP-DOE AMIP-II reanalysis (R-2), Bull. Amer. Meteor. Soc., 83, 1631–1643, https://doi.org/10.1175/BAMS-83-11-1631, 2002.

Kim, J. E., and Hong, S. Y.: Impact of soil moisture anomalies on summer rainfall over east Asia: a regional climate model study, J. Clim., 20, 5732–5743, https://doi.org/10.1175/2006jcli1358.1, 2007.

Komma, J., Blöschl, G., and Reszler, C.: Soil moisture updating by Ensemble Kalman Filtering in real-time flood forecasting, J. Hydrol., 357, 228–242, https://doi.org/10.1016/j.jhydrol.2008.05.020, 2008.

Lai, X., Wen, J., Ceng, S. X., Song, H. Q., Tian, H., Shi, X. K., He, Y., and Huang, X.: Numerical simulation and evaluation study of soil moisture over China by using CLM4.0 model, J. Atmos. Sci., 38, 499–512, 2014.

Li, H. Y., Robock, A., Liu, S., Mo, X., and Viterbo, P.: Evaluation of reanalysis soil moisture simulations using updated Chinese soil moisture observations, J. Hydrometeorol., 6, 180–193, https://doi.org/10.1175/jhm416.1, 2009.

https://doi.org/10.5194/hess-2020-611
Preprint. Discussion started: 4 January 2021

Li, M., Wu, P., and Ma, Z.: A comprehensive evaluation of soil moisture and soil temperature from third-generation atmospheric and land reanalysis data sets, Int. J. Climatol., 40, 5744–5766, https://doi.org/10.1002/joc.6549, 2020.

Li, Y., Li, Y., Yuan, X., Zhang, L., and Sha, S.: Evaluation of model-based soil moisture drought monitoring over three key regions in China, J. Appl. Meteorol. Climatol., 57, 1989–2004, https://doi.org/10.1175/jamc-d-17-0118.1, 2018.

Liu, L., Zhang, R., and Zuo, Z.: Intercomparison of spring soil moisture among multiple reanalysis data sets over eastern China, J. Geophys. Res., 119, 54–64, https://doi.org/10.1002/2013jd020940, 2014.

Liu, Y. Y., Dorigo, W. A., Parinussa, R. M., de Jeu, R. A. M., Wagner, W., McCabe, M. F., Evans, J. P., and van Dijk, A. I. J. M.: Trend-preserving blending of passive and active microwave soil moisture retrievals, Remote Sens. Environ., 123, 280–297, https://doi.org/10.1016/j.rse.2012.03.014, 2012.

Ma, S., Zhu, K., Li, M., and Ma, Z.: A comparative study of multi-source soil moisture data for China's regions, Clim. Environ. Res., 21, 121–133, https://doi.org/10.3878/j.issn.1006-9585.2015.15080, 2016.

Markewitz, D., Devine, S., Davidson, E. A., Brando, P., and Nepstad, D. C.: Soil moisture depletion under simulated drought in the Amazon: impacts on deep root uptake, New Phytol., 187, 592–607, https://doi.org/10.1111/j.1469-8137.2010.03391.x, 2010.

McColl, K. A., Wang, W., Peng, B., Akbar, R., Gianotti, D. J. S., Lu, H., Pan, M., and Entekhabi, D.: Global characterization of surface soil moisture drydowns, Geophys. Res. Lett., 44, 3682–3690, https://doi.org/10.1002/2017gl072819, 2017.

Data set of crop growth and soil moisture in China (AGME_AB2_CHN_TEN): http://data.cma.cn/data/cdcdetail/dataCode/AGME_AB2_CHN_TEN.html, last access: 27 November 2017, 2006.

Norbiato, D., Borga, M., Esposti, S. D., Gaume, E., and Anquetin, S.: Flash flood warning based on rainfall thresholds and soil moisture conditions: an assessment for gauged and ungauged basins, J. Hydrol., 362, 274–290, https://doi.org/10.1016/j.jhydrol.2008.08.023, 2008.

Ochsner, T. E., Cosh, M. H., Cuenca, R. H., Dorigo, W. A., Draper, C. S., Hagimoto, Y., Kerr, Y. H., Larson, K. M., Njoku, E. G., Small, E. E., and Zreda, M.: State of the art in large-scale soil moisture monitoring, Soil Sci. Soc. Am. J., 77, 1888–1919, https://doi.org/10.2136/sssaj2013.03.0093, 2013.

The ERA-interim archive version 2.0: https://apps.ecmwf.int/datasets/data/interim-full-daily/levtype=sfc/, last access: 5 June 2018, 2011.

Peng, J., Niesel, J., Loew, A., Zhang, S., and Wang, J.: Evaluation of satellite and reanalysis soil moisture products over southwest China using ground-based measurements, Remote Sens., 7, 15729–15747, https://doi.org/10.3390/rs71115729, 2015.

Peng, J., and Loew, A.: Recent advances in soil moisture estimation from remote sensing, Water, 9, 530, https://doi.org/10.3390/w9070530, 2017.

Peng, J., Loew, A., Merlin, O., and Verhoest, N. E. C.: A review of spatial downscaling of satellite remotely sensed soil moisture, Rev. Geophys., 55, 341–366, https://doi.org/10.1002/2016RG000543, 2017.

https://doi.org/10.5194/hess-2020-611
Preprint. Discussion started: 4 January 2021

Petropoulos, G. P., Ireland, G., and Barrett, B.: Surface soil moisture retrievals from remote sensing: current status, products & future trends, Phys. Chem. Earth Parts A/B/C, 83-84, 36–56, https://doi.org/10.1016/j.pce.2015.02.009, 2015.

Qiu, B., Xue, Y., Fisher, J. B., Guo, W., Berry, J. A., and Zhang, Y.: Satellite chlorophyll fluorescence and soil moisture observations lead to advances in the predictive understanding of global terrestrial coupled carbon-water cycles, Glob. Biogeochem. Cycles, 32, 360–375, https://doi.org/10.1002/2017gb005744, 2018.

Robock, A., Vinnikov, K. Y., Srinivasan, G., Entin, J. K., Hollinger, S. E., Speranskaya, N. A., Liu, S., and Namkhai, A.: The global soil moisture data bank, Bull. Am. Meteorol. Soc., 81, 1281–1299, https://doi.org/10.1175/1520-0477(2000)081<1281:tgsmdb>2.3.co;2, 2000.

Schellekens, J., Dutra, E., Martínez-de la Torre, A., Balsamo, G., van Dijk, A., Weiland, F. S., Minvielle, M., Calvet, J.-C., Decharme, B., Eisner, S., Fink, G., Flörke, M., Peßenteiner, S., van Beek, R., Polcher, J., Beck, H., Orth, R., Calton, B., Burke, S., Dorigo, W., and Weedon, G. P.: A global water resources ensemble of hydrological models: the eartH2Observe Tier-1 dataset, Earth Syst. Sci. Data, 9, 389–413, https://doi.org/10.5194/essd-9-389-2017, 2017.

Seneviratne, S. I., Corti, T., Davin, E. L., Hirschi, M., Jaeger, E. B., Lehner, I., Orlowsky, B., and Teuling, A. J.: Investigating soil moisture–climate interactions in a changing climate: a review, Earth Sci. Rev., 99, 125–161, https://doi.org/10.1016/j.earscirev.2010.02.004, 2010.

Sevanto, S., McDowell, N. G., Dickman, L. T., Pangle, R., and Pockman, W. T.: How do trees die? A test of the hydraulic failure and carbon starvation hypotheses, Plant Cell Environ., 37, 153–161, https://doi.org/10.1111/pce.12141, 2014.

Shrivastava, S., Kar, S. C., and Sharma, A. R.: Soil moisture variations in remotely sensed and reanalysis datasets during weak monsoon conditions over central India and central Myanmar, Theor. Appl. Climatol., 129, 305–320, https://doi.org/10.1007/s00704-016-1792-z, 2017.

Wells, N., Goddard, S., and Hayes, M. J.: A self-calibrating palmer drought severity index, J. Clim., 17, 2335–2351, https://doi.org/10.1175/1520-0442(2004)017<2335:aspdsi>2.0.co;2, 2004.

Western, A. W., and Blöschl, G.: On the spatial scaling of soil moisture, J. Hydrol., 217, 203–224, https://doi.org/10.1016/s0022-1694(98)00232-7, 1999.

Wu, J. and Gao, X. J.: A gridded daily observation dataset over China region and comparison with the other datasets, Chinese J. Geophys. (in Chinese), 56(4), 1102-1111, https://doi.org/10.6038/cjg20130406, 2013.

Yang, K., He, J., Tang, W., Qin, J., and Cheng, C. C. K.: On downward shortwave and longwave radiations over high altitude regions: observation and modeling in the Tibetan Plateau, Agric. For. Meteorol., 150, 38–46, https://doi.org/10.1016/j.agrformet.2009.08.004, 2010.

Zhang, W., Zhou, T., and Zhi, H.: Numerical test of soil moisture affecting summer climate in China, J. Meteorol., 70, 78–90, https://doi.org/10.1007/s11783-011-0280-z, 2012.

Zhu, Z., Shi, C., Zhang, T., and Wang, J.: Applicability analysis of four reanalysis soil moisture datasets in China, Plateau Meteorol., 37, 240–252, https://doi.org/10.7522/j.issn.1000-0534.2017.00033, 2018.

https://doi.org/10.5194/hess-2020-611
Preprint. Discussion started: 4 January 2021

Hydrology and Earth System Sciences
Discussions

Zuo, Z., and Zhang, R.: Soil Moisture and its Impact on the East Asian Summer Monsoon, American Geophysical Union, Washington, DC, 2016.

https://doi.org/10.5194/hess-2020-611
Preprint. Discussion started: 4 January 2021

Hydrology and Earth System Sciences
Discussions

Figure Captions

Figure 1: Spatial distribution of 119 agricultural-meteorological observation stations and four research regions over China for the period 1981 to 2013. The colors denote the distribution of annual precipitation (unit: mm/year) from 1971-2000.

Figure 2: Annual averages of (a) observations and (b~e) five satellite/reanalysis SM products (units: $m^3 \cdot m^{-3}$) during June to August for the period of 1981 to 2013 in China.

Figure 3: The rRMSEs of (a) observations and (b~e) four satellite/reanalysis SM products (units: $m^3 \cdot m^{-3}$) during April to September for the period of 1981 to 2013 in China.

Figure 4: Time series of SM in four research regions (a~d) from 1981 to 2013.

Figure 5: Taylor diagrams of the comparison between multisource SM products and in situ observations. Ref. is the SM from in situ observations.

Figure 6: Seasonality of SM distributions based on in situ observations and five products averaged over the (a) NE, (b) NC, (c) YH, and (d) NW regions from 1981 to 2013.

Figure 7: Distribution of autocorrelation coefficient of SM in seasons: (1st row) FMA and MAM; (2nd row) MJJ and JJA; (3rd row) ASO and SON; (4th row) NDJ and DJF.

Figure 8: Temporal evolution of the JJA SM anomaly time series from observations and the five satellite/reanalysis products in four research regions from 1981 to 2013.

Figure 9: Contributions of three terms to the mean square errors (MSEs) for the four satellite/reanalysis products from 1981 to 2013.

Figure 10: Evaluation of remote sensing and reanalysis SM against in situ observations under dry or wet conditions.

Figure 11: Evaluation of remote sensing and reanalysis SM against in situ observations under dry or wet conditions in different regions.

Figure 12: Scatterplots of monthly anomalies of (a) precipitation, (b) temperature, and (c) net radiation vs observed soil moisture in the top 10 cm depth during 1981-2013. R is the correlation coefficient in over four research regions.

https://doi.org/10.5194/hess-2020-611
Preprint. Discussion started: 4 January 2021


Hydrology and Earth System Sciences
Discussions

560 **Tables**

Table 1: Details of the SM products used in the study.

Name	Soil Depths (cm)	Spatial Resolution	Temporal Resolution	Temporal Coverage
		In situ		
OBS	10, 20, 50, 70, 100	778 stations (119 used)	3x monthly	1981.01-2013.12
		Satellite		
ESA CCI	~ 2-5	0.25°*0.25°	Daily, monthly	1978.11-present
		Reanalysis		
ERAI	0-7, 7-28, 28-100, 100-255	0.75°*0.75°	4x daily, monthly	1979.01-present
NCEP	0-10, 10-200	T62 (~2°*2°)	4x daily, monthly	1979.01-present
NOAA	0, 10, 40, 100	2°*2°	8x daily, monthly	1851.01-2014.12
ERA5	0-7, 7-28, 28-100, 100-255	0.28125°*0.28125°	2x daily, monthly	1979.01-present

https://doi.org/10.5194/hess-2020-611
Preprint. Discussion started: 4 January 2021

Hydrology and Earth System Sciences
Discussions

Table 2: Names and spatial coverage of the selected research regions.

		Regions	Zonal Coverage (°E)	Meridional Coverage (°N)
I	NE	Northeast	118~130	39.5~50.5
II	NC	North China	110~117.5	34.5~42
III	YH	YH	110~120	29.5~34.5
IV	NW	Northwest	99.5~110	32.5~41

https://doi.org/10.5194/hess-2020-611
Preprint. Discussion started: 4 January 2021

Hydrology and Earth System Sciences
Discussions

565 **Table 3: Correlation coefficients, biases and RMSEs of the five datasets for JJA SM from 1981 to 2013. The coefficients in brackets are those that cannot pass the significance test (α=0.01) with n=33.**

Regions	Products	Bias	RMSE	Correlation
Northeast	ESA CCI	0.001	0.009	-0.119
	NCEP	0.079	0.009	0.307
	ERAI	0.073	0.027	0.419
	NOAA/CIRES 20CR	0.145	0.016	0.460
	ERA5	0.121	0.021	0.481
North China	ESA CCI	-0.004	0.021	0.023
	NCEP	0.062	0.007	0.140
	ERAI	0.058	0.024	0.485
	NOAA/CIRES 20CR	0.101	0.018	0.221
	ERA5	0.054	0.023	0.616
Yangtze-Huai	ESA CCI	-0.019	0.020	0.114
	NCEP	0.071	0.009	0.453
	ERAI	0.067	0.024	0.466
	NOAA/CIRES 20CR	0.134	0.024	0.427
	ERA5	0.097	0.028	0.504
Northwest	ESA CCI	-0.028	0.012	0.169
	NCEP	0.055	0.008	(-0.080)
	ERAI	0.039	0.019	(0.000)
	NOAA/CIRES 20CR	0.058	0.011	(-0.035)
	ERA5	0.030	0.020	0.158

https://doi.org/10.5194/hess-2020-611
Preprint. Discussion started: 4 January 2021

Hydrology and Earth System Sciences
Discussions

Figures

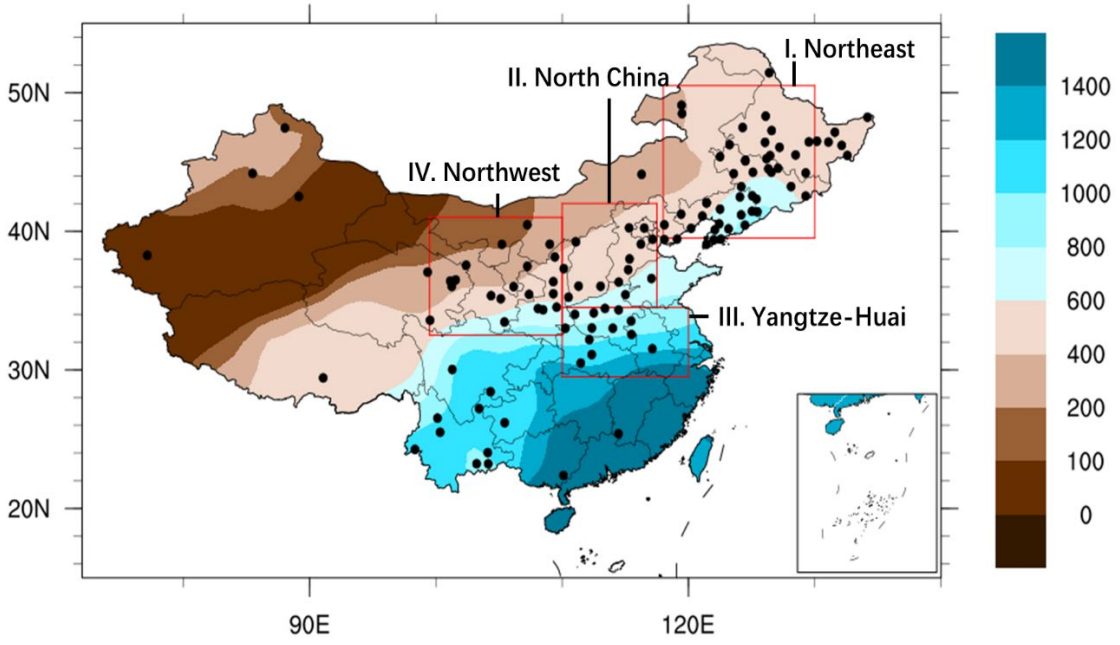

570 **Figure 1. Spatial distribution of 119 agricultural-meteorological observation stations and four research regions over China for the period 1981 to 2013. The colors denote the distribution of annual precipitation (unit: mm/year) from 1971-2000.**

https://doi.org/10.5194/hess-2020-611
Preprint. Discussion started: 4 January 2021

Hydrology and Earth System Sciences
Discussions

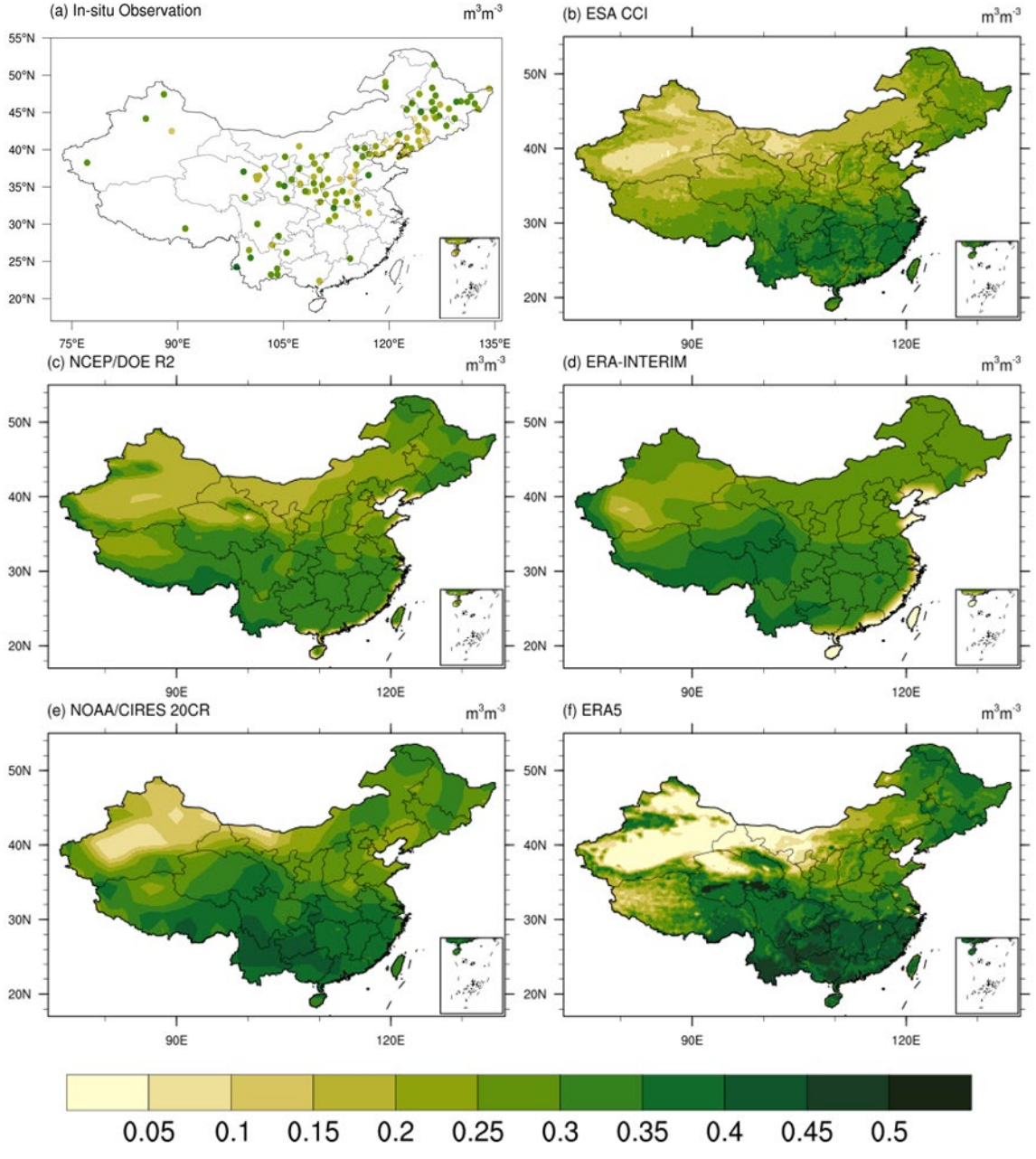

Figure 2. Annual averages of (a) observations and (b~e) five satellite/reanalysis SM products (units: $m^3 \cdot m^{-3}$) during June to August for the period of 1981 to 2013 in China.

https://doi.org/10.5194/hess-2020-611
Preprint. Discussion started: 4 January 2021

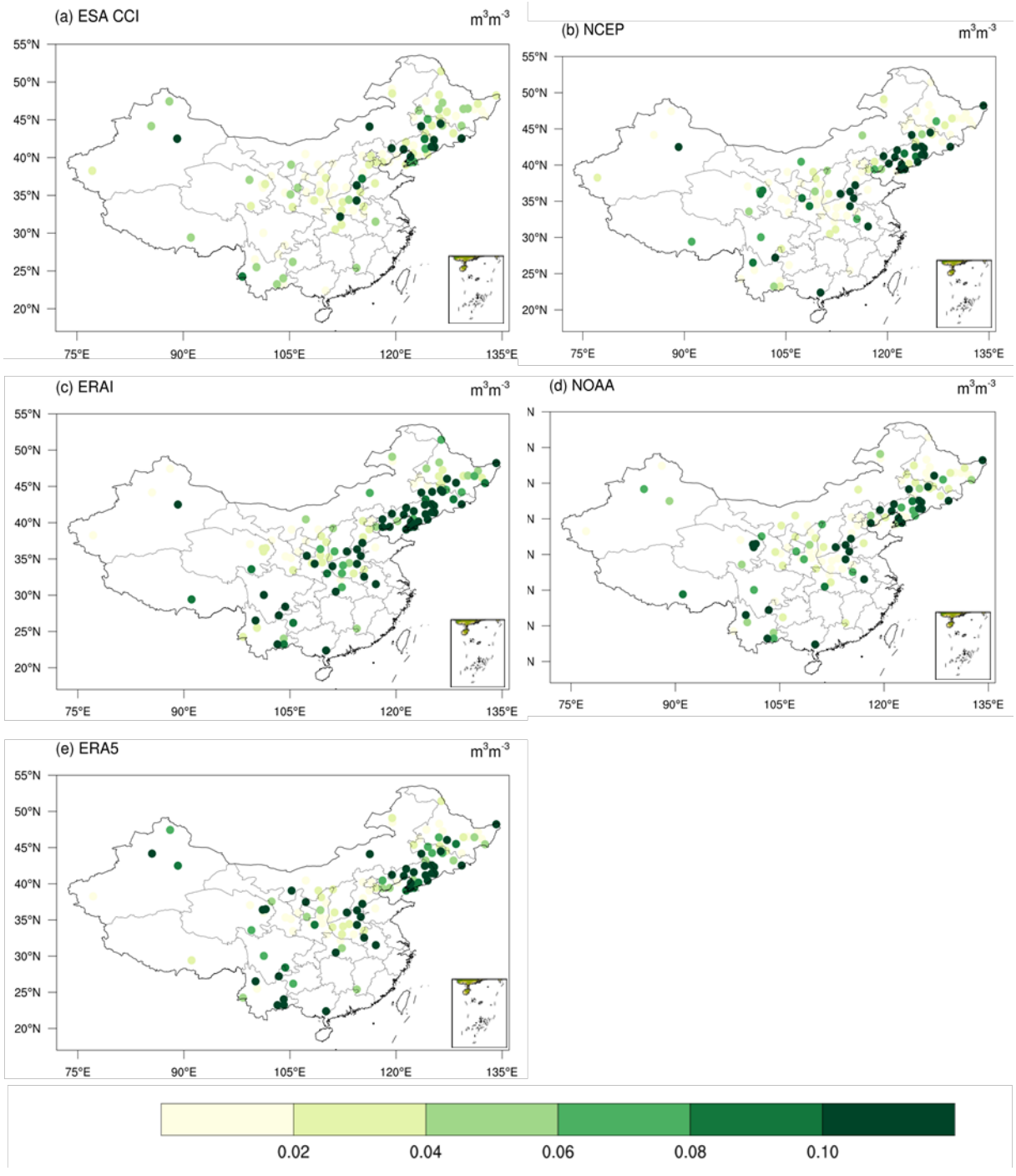

Figure 3. Same as Figure 2 but for rRMSE.

https://doi.org/10.5194/hess-2020-611
Preprint. Discussion started: 4 January 2021

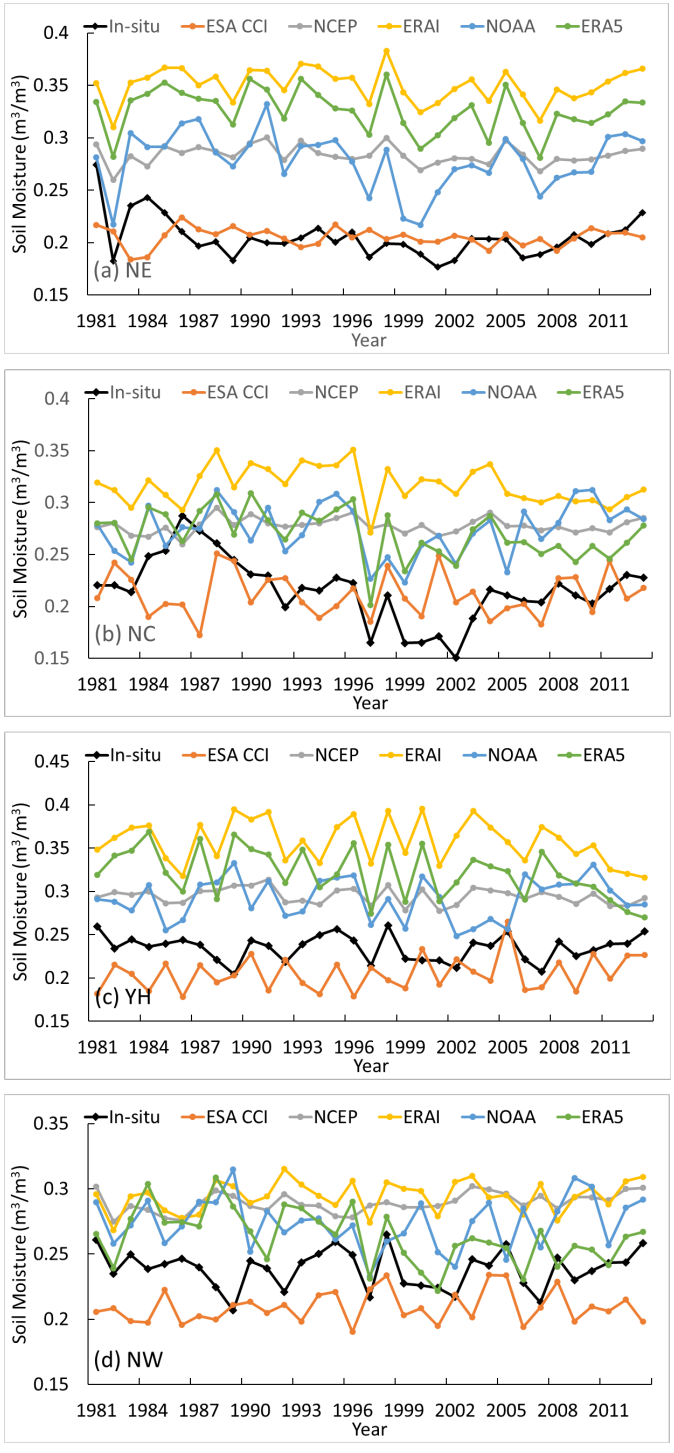

580 **Figure 4. Time series of SM in four research regions (a~d) from 1981 to 2013.**

https://doi.org/10.5194/hess-2020-611
Preprint. Discussion started: 4 January 2021

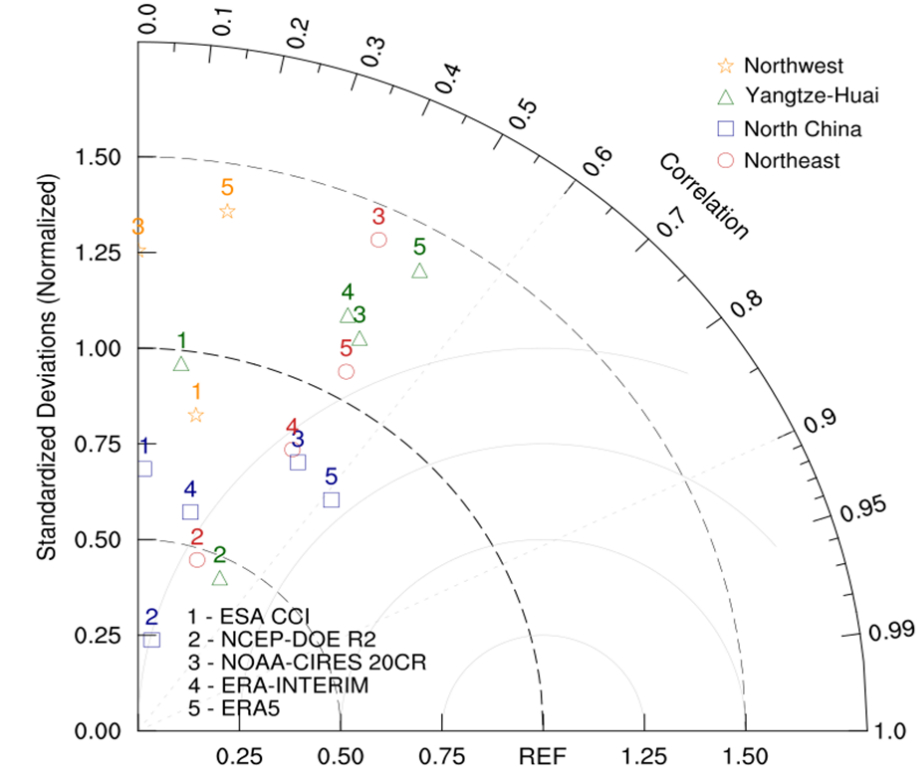

Figure 5. Taylor diagrams of the comparison between multisource SM products and in situ observations. Ref. is the SM from in situ observations.

https://doi.org/10.5194/hess-2020-611
Preprint. Discussion started: 4 January 2021

Hydrology and Earth System Sciences
Discussions

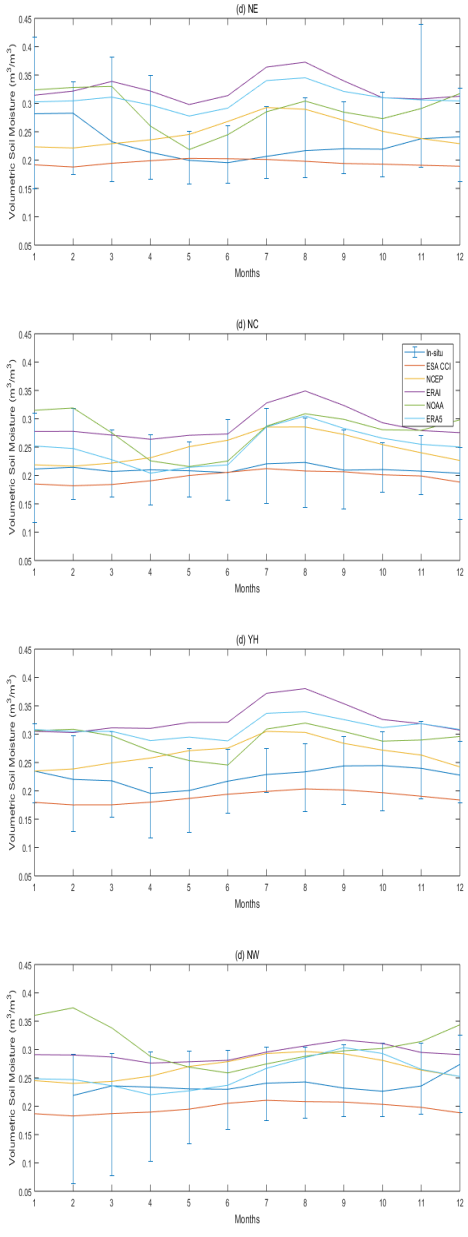

Figure 6. Seasonality of SM distributions based on in situ observations and five products averaged over the (a) NE, (b) NC, (c) YH, and (d) NW regions from 1981 to 2013.

590

https://doi.org/10.5194/hess-2020-611
Preprint. Discussion started: 4 January 2021

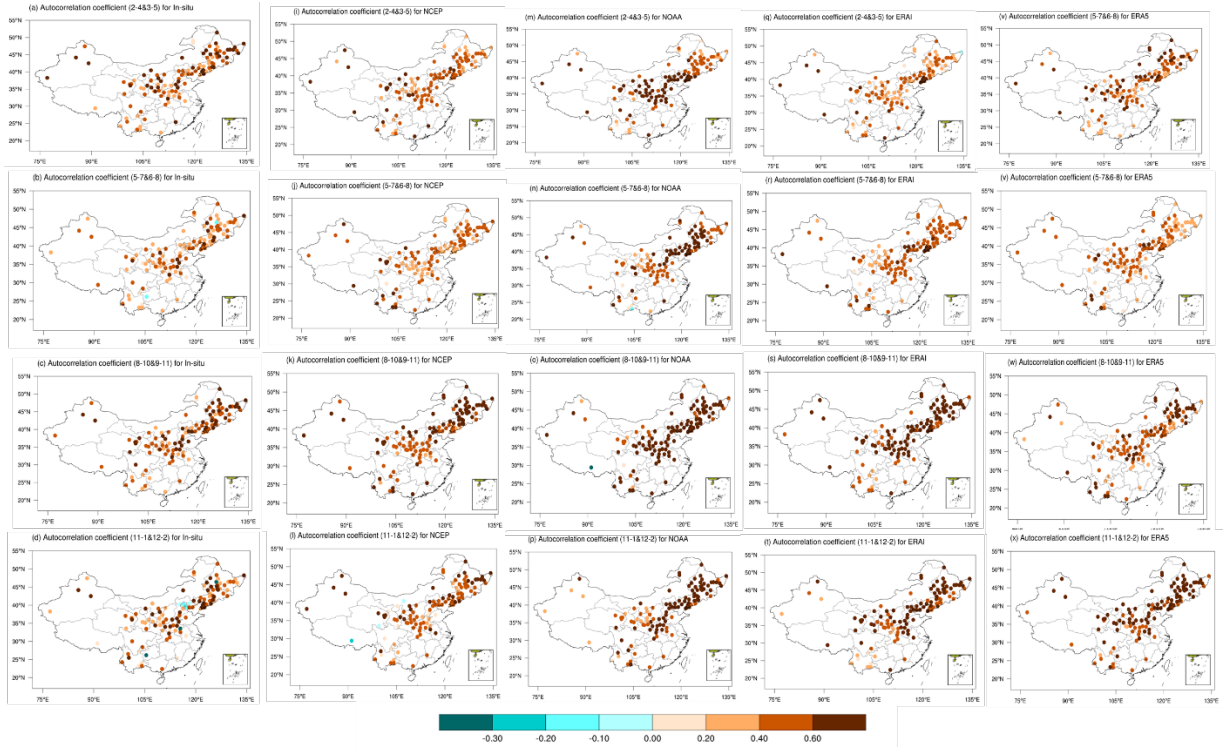

Figure 7. Distribution of autocorrelation coefficient of SM in seasons: (1st row) FMA and MAM; (2nd row) MJJ and JJA; (3rd row) ASO and SON; (4th row) NDJ and DJF.

https://doi.org/10.5194/hess-2020-611
Preprint. Discussion started: 4 January 2021

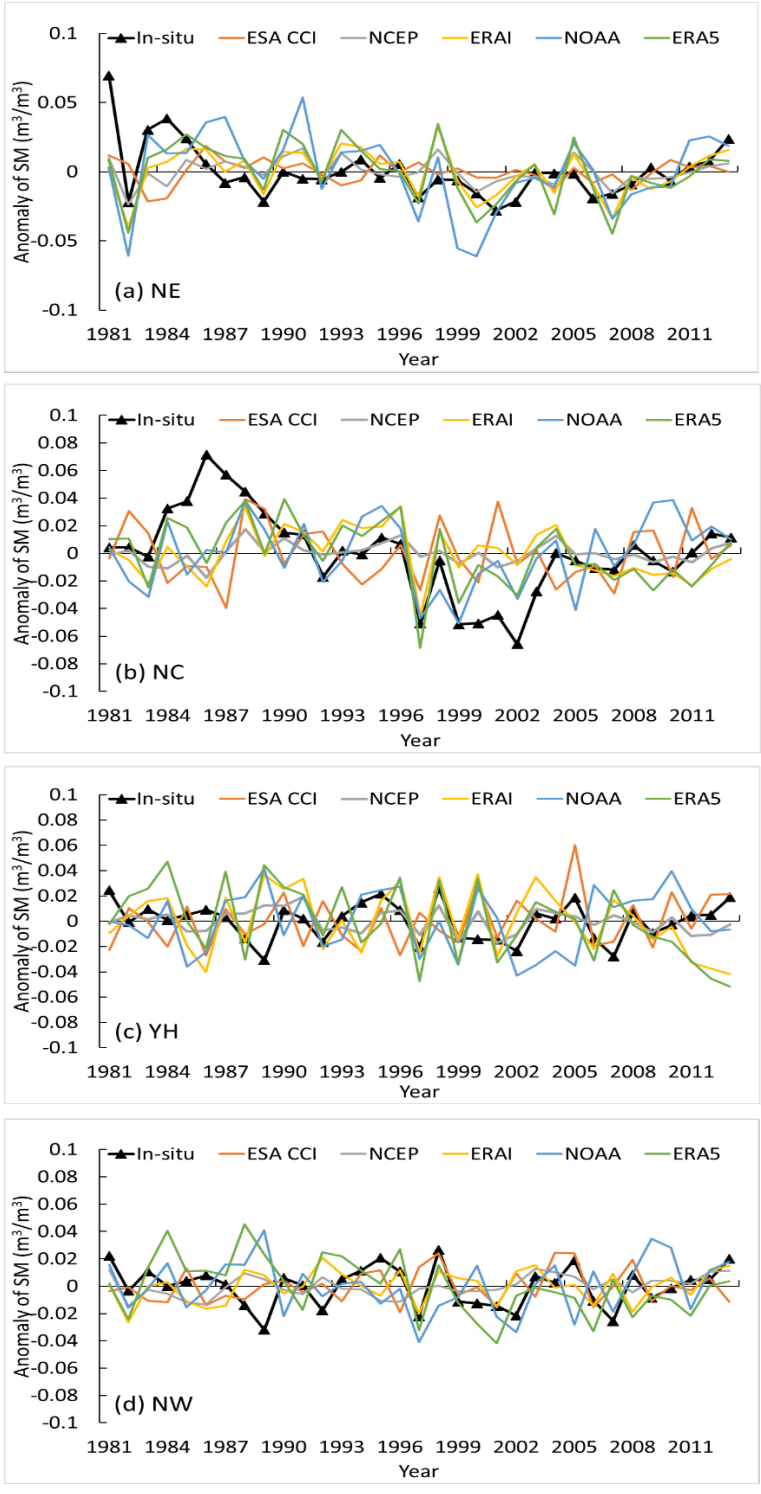

595

Figure 8. Temporal evolution of the JJA SM anomaly time series from observations and the five satellite/reanalysis products in four research regions from 1981 to 2013.

https://doi.org/10.5194/hess-2020-611
Preprint. Discussion started: 4 January 2021

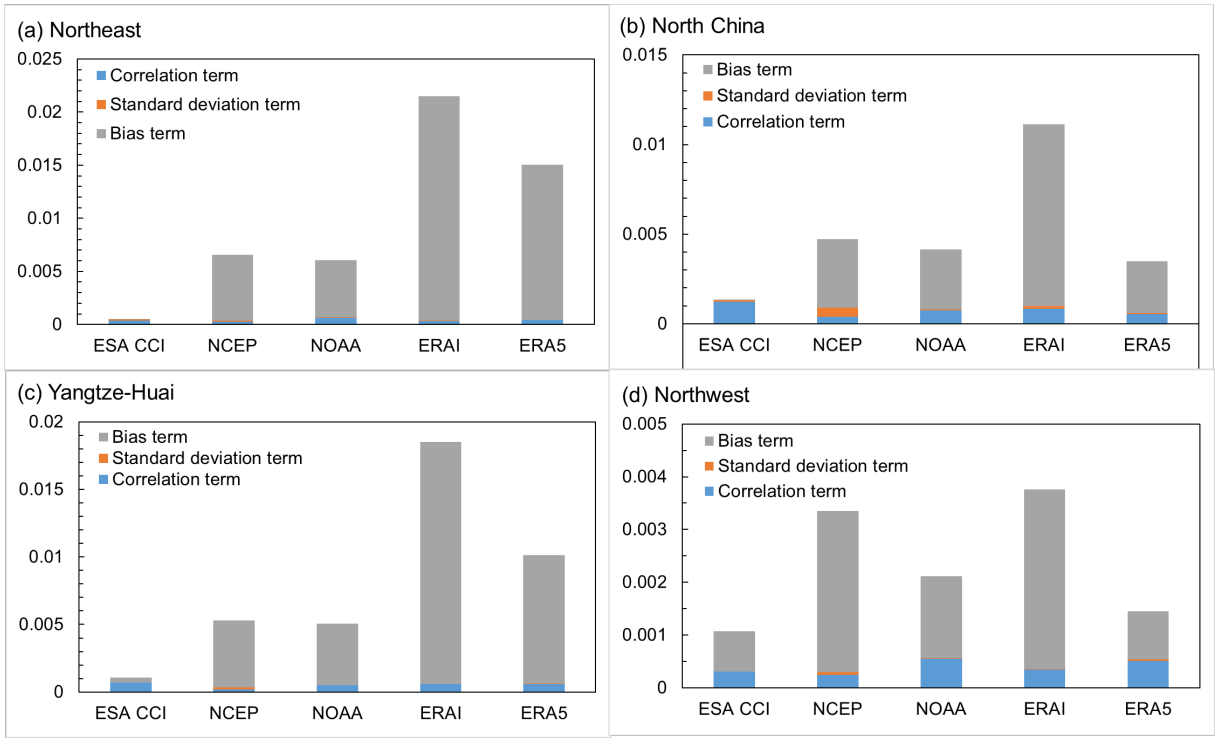

Figure 9. Contributions of three terms to the mean square errors (MSEs) for the four satellite/reanalysis products from 1981 to 2013.

600

https://doi.org/10.5194/hess-2020-611
Preprint. Discussion started: 4 January 2021

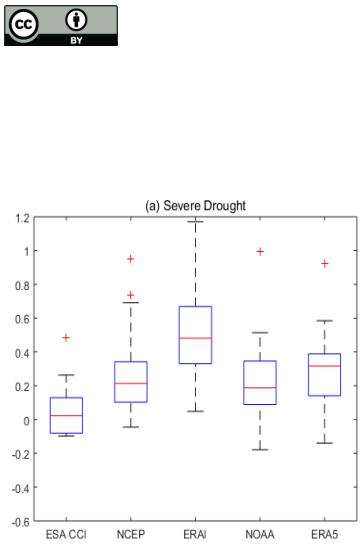

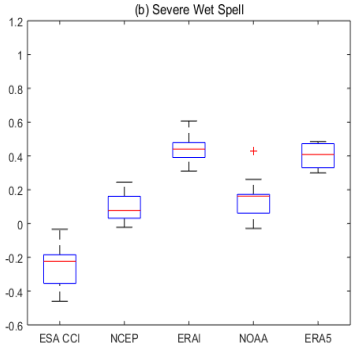

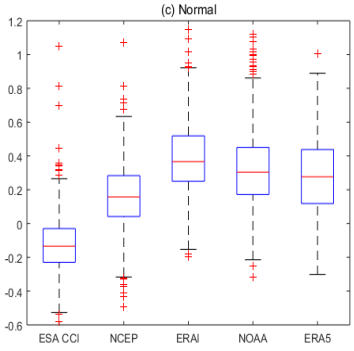

Figure 10. Evaluation of remote sensing and reanalysis SM against in situ observations under dry or wet conditions.

https://doi.org/10.5194/hess-2020-611
Preprint. Discussion started: 4 January 2021

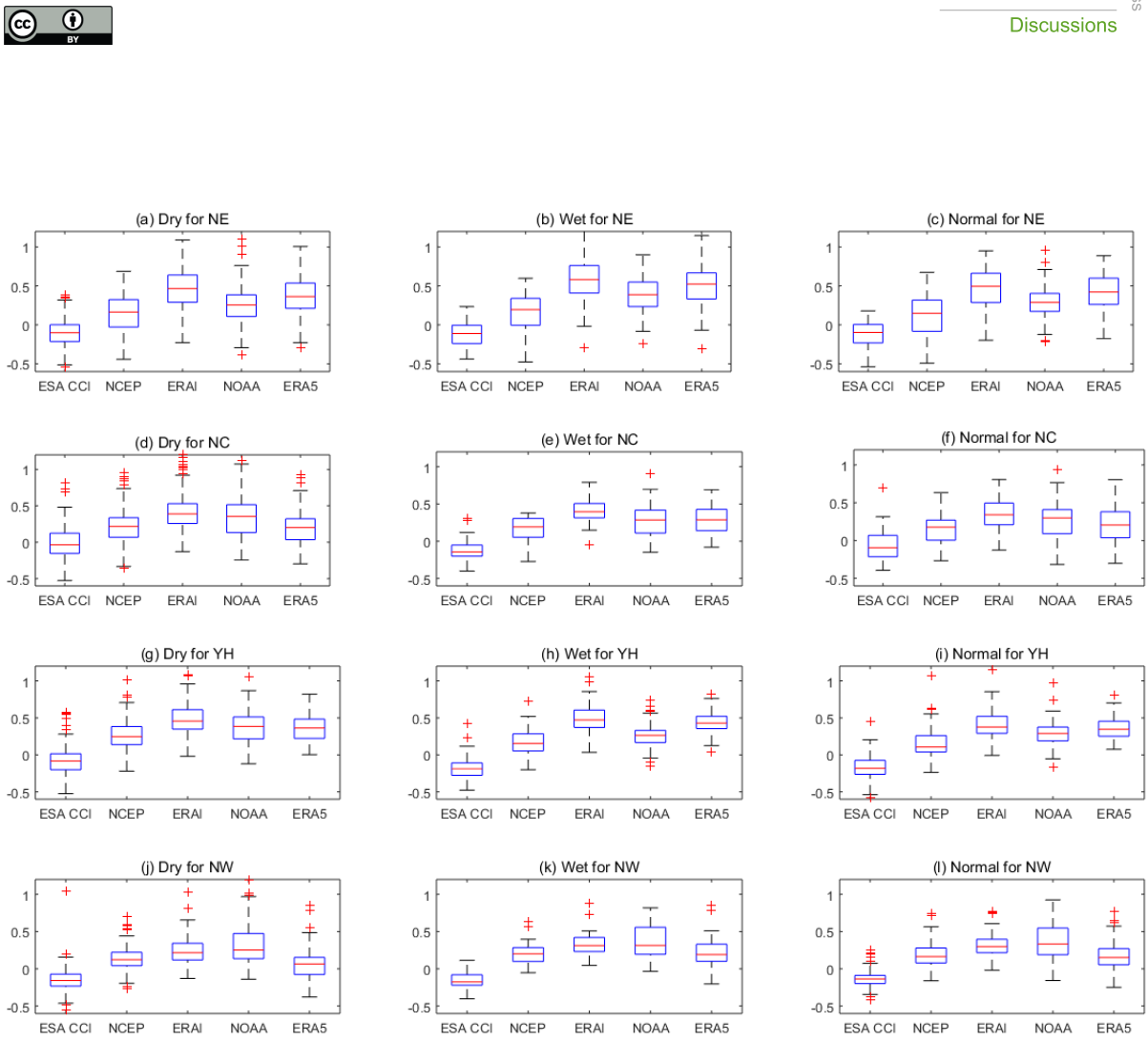

Figure 11. Evaluation of remote sensing and reanalysis SM against in situ observations under dry or wet conditions in different regions.

https://doi.org/10.5194/hess-2020-611
Preprint. Discussion started: 4 January 2021

Hydrology and Earth System Sciences
Discussions

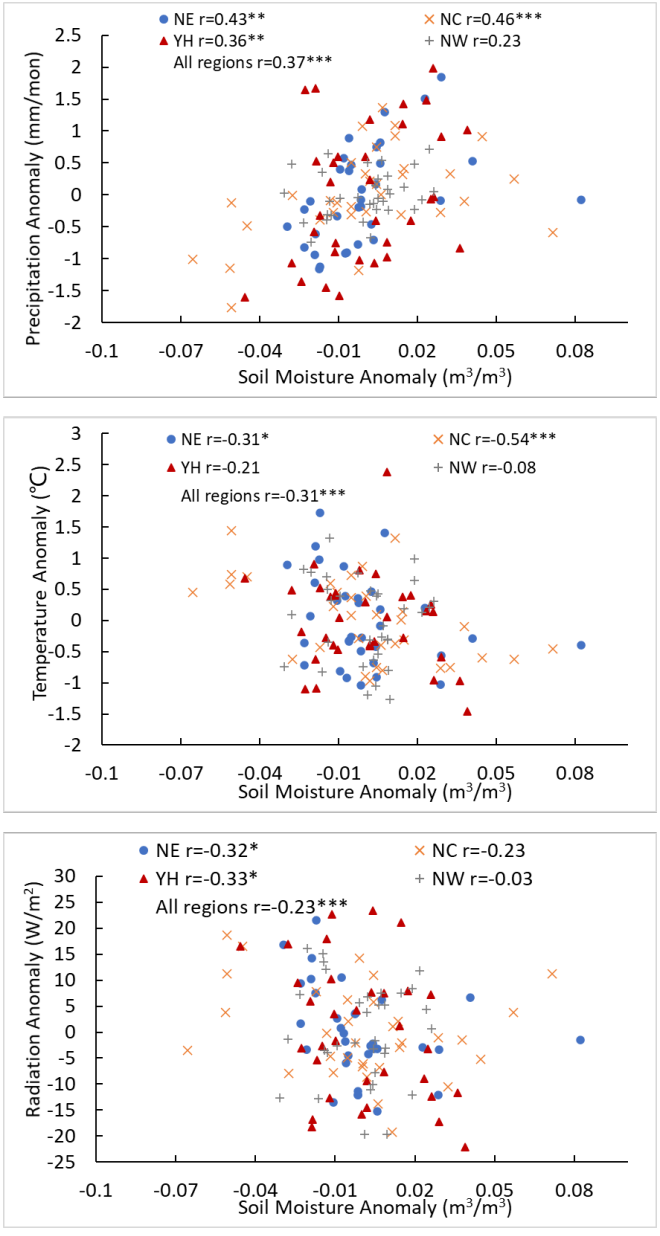

Figure 12. Scatterplots of monthly anomalies of (a) precipitation, (b) temperature, and (c) net radiation vs observed soil moisture in the top 10 cm depth during 1981-2013. R is the correlation coefficient in over four research regions.